Journal of Organometallic Chemistry 1000 (2023) 122844

Contents lists available at ScienceDirect

Journal of Organometallic Chemistry

journal homepage: www.elsevier.com/locate/jorganchem

Effect of β-cyclodextrin on the CO release kinetics and antimicrobial activity of $[NEt_4][Mo(CO)_5Br]$

Rodrigo P. Monteiro [a,1], Isabel B. Calhau [a,1], Ana C. Gomes [a], Carla Pereira [b], Cátia Vieira [b], M. Amparo F . Faustino [c], Adelaide Almeida [b,*], Martyn Pillinger [a], Carlos C. Romão [d], Isabel S. Gonçalves [a,*]

[a] CICECO - Aveiro Institute of Materials, Department of Chemistry, University of Aveiro, Campus Universitário de Santiago, 3810-193 Aveiro, Portugal
[b] CESAM - Centre for Environmental and Marine Studies, Department of Biology, University of Aveiro, Campus Universitário de Santiago, 3810-193 Aveiro, Portugal
[c] LAQV-Requimte & Department of Chemistry, University of Aveiro, Campus Universitário de Santiago, 3810-193 Aveiro, Portugal
[d] Instituto de Tecnologia Química e Biológica António Xavier, Universidade Nova de Lisboa, Oeiras, Portugal

ARTICLE INFO

Keywords:
Carbon monoxide-releasing molecules
β-cyclodextrin
Mb assay
Antibacterial activity
Escherichia coli

ABSTRACT

In the present work the possibility of improving the solubility, bioavailability and bactericidal activity of the carbon monoxide releasing molecule (CORM) $[Mo(CO)_5Br]^-$ (as its tetraethylammonium salt) (**1**) by solvent-free co-grinding with β-cyclodextrin (βCD) in a planetary ball mill was investigated. Data obtained by FT-IR spectroscopy, Raman spectroscopy, powder X-ray diffraction and thermogravimetric analysis showed that, other than a small decrease in the crystallinity of **1**, the co-grinding process produced a finely dispersed physical mixture of crystalline CORM and crystalline excipient. The aqueous solubility of **1** in the **1**-βCD product was enhanced with respect to sparingly soluble pure **1**, which might be ascribed to increased wettability and a CD-CORM interaction in solution. Investigation of the CO release kinetics by the standard myoglobin assay showed that the half-life of CO release increased from ca. 6 min for **1** to ca. 19 min for **1**-βCD, while the number of equivalents released decreased from 3.2 to 1.8. The antibacterial properties of **1** and **1**-βCD were evaluated using the broth microdilution method to determine minimum inhibitory concentration (MIC) and minimum bactericidal concentration (MBC) against the model Gram-negative bacterium, *Escherichia coli*. The compounds showed similar growth inhibitory (MIC values of 200 μM) and bactericidal (MBC/MIC ≈ 2) effects. Bacterial viability assays corroborated the MBC/MIC studies, showing 3 logs (99.9% of relative light units - RLU) reduction in viable cell count after 15 min exposure to 2 × MIC. Although the CORM-CD system displays a lengthening of the half-life of CO release and a decrease in the CO release efficiency relative to **1**, the co-grinding with βCD does not affect the bactericidal activity of the CORM. Overall, the βCD could be a suitable excipient for the development of immediate-release formulations of CORMs like the pentacarbonyl complex **1**.

1. Introduction

Experimental evidence for the endogenous production of carbon monoxide (CO), via oxidative metabolism of heme, was obtained by Sjöstrand in the middle of the twentieth century [1]. In 1968, Tenhunen et al. showed that the reaction was enzymatic in nature, i.e., catalyzed by heme oxygenase, yielding CO, biliverdin, and free ferrous iron [2]. Despite these momentous discoveries, the image of CO as a lethal, toxic gas, persisted for many years, and it was only in 1991 that a physiological role was hypothesized [3]. Two years later, the suggestion that CO may function as a neurotransmitter [4] spurred an extensive investigation of the biological roles and mechanisms of action of CO, which firmly established the gas as an essential signaling molecule and a potential therapeutic agent for the treatment of various conditions such as rheumatoid arthritis, gastric ulcers, sepsis, lung injury, cardiovascular disease, stroke, transplant rejection, and cancer [5,6].

Following successful preclinical animal studies with inhaled CO (iCO) [7,8], clinical trials were initiated from about 2004 onwards to examine safety, tolerability and efficacy in humans [8–11]. Administration of low-dose iCO (that results in carboxyhemoglobin (COHb)

* Corresponding authors.
E-mail addresses: aalmeida@ua.pt (A. Almeida), igoncalves@ua.pt (I.S. Gonçalves).
[1] These authors contributed equally.

https://doi.org/10.1016/j.jorganchem.2023.122844
Received 26 June 2023; Received in revised form 28 July 2023; Accepted 30 July 2023
Available online 1 August 2023

levels up to about 10%) has been shown to be feasible, well tolerated and safe in healthy volunteers and patients with ailments such as chronic lung disease and acute respiratory distress syndrome. Limitations of low-dose iCO therapy include lack of targetability, requirement to be performed in a hospital setting, and high dependence of the outcome on the respiratory function of the patient [9]. To sidestep these issues, Motterlini and coworkers proposed CO-releasing molecules (CORMs) as pharmaceutical agents for the controlled delivery of CO to tissues and organs [12]. The first CORMs were the metal carbonyls $[Mn_2(CO)_{10}]$ (CORM-1), $[\{Ru(CO)_3Cl_2\}_2]$ (CORM-2) and $[Ru(CO)_3Cl(glycinate)]$ (CORM-3) [13,14], and the boronocarbonate $Na_2[H_3BCO_2]$ (CORM-A1) [15]. Most preclinical efficacy studies to date have focused on these CORMs [8]. While water-insoluble CORM-1 requires exposure to light to release CO (and was therefore the first photoactivated CORM, commonly abbreviated as photoCORM), CORM-3 releases CO immediately upon dissolution in aqueous media through a hydrolytic trigger, and CORM-A1 displays pH- and temperature-dependent CO release. Over the last two decades, CORM development has expanded greatly to include a wide variety of organometallic complexes (M = Ru, Fe, Mn, V, Co, Ir, Cr, Mo, W) [16–19], metal-free organic CO-prodrugs [20,21], photoCORMs [22,23], and CO-releasing materials [24,25].

One of the hurdles in using metal carbonyl complexes as CO-prodrugs is the development of formulation strategies that improve the stability, handling, aqueous solubilities, and dissolution rates (and hence bioavailabilities) of the complexes. One approach is to incorporate functional excipients in the formulation to assist in the dissolution process of the drug [26,27]. Cyclodextrins (CDs) are among the most widely used and pharmaceutically acceptable excipients [28–30] because of their safe toxicological profile, ability to solubilize poorly soluble drugs, and aptness for solvent-free co-grinding [31], which is one of the most common manufacturing techniques used in the pharmaceutical industry. The best-known characteristic of CDs is their ability to form noncovalent inclusion complexes with hydrophobic molecules or lipophilic moieties thereof [32]. CDs can also form non-inclusion complexes or self-assembled nanoaggregates (sustained by CD-guest or CD-CD hydrogen bonding interactions involving the hydroxyl groups on the outer surface of the CD) that present an enhanced water solubility and stability [33,34]. Even intimate physical mixtures, prepared by co-grinding, may display marked increases in the dissolution rate due to the positive effect of CDs on the wettability of hydrophobic drug molecules, and an in situ inclusion process promoted by the rapid dissolution of the CD in the aqueous environment [35].

The first CORMs were widely studied in models of inflammation, vascular dysfunction, cardiovascular disease, ischemic injury, and organ transplantation. Among them, an early study described the strong anti-inflammatory activity of the pentacarbonyl complex $[Et_4N][Mo(CO)_5Br]$ (ALF062) in animal models of disease [36]. Interestingly, and somewhat unexpectedly, some of these CORMs exhibited antimicrobial activity against several bacterial targets in vitro and in animal models of infection [37,38]. A seminal study by Nobre et al. showed that CORM-2, CORM-3 and $[Et_4N][Mo(CO)_5Br]$ decreased the viability of Gram-negative *E. coli* and Gram-positive *Staphylococcus aureus*, grown either under aerobic or anaerobic conditions, while being nontoxic to eukaryotic cells under similar conditions [39]. Confirmation that the antimicrobial action of the CORMs was dependent on their release of CO was obtained by the finding that the bactericidal effect was completely lost when the antibacterial experiments were performed in the present of the CO scavenger hemoglobin. It was subsequently proposed that the bactericidal effects were due to reactive oxygen species (ROS) generated by the CORMs in a CO-dependent manner [40]. In general, the mode of action of antimicrobial CORMs must be considered on a case-by-case basis to establish whether the antibacterial performance derives from the released CO, the metal ions, the CORM scaffold, or the metal fragments that are generated intracellularly upon CO release [41].

Now that the efficacy of CORMs as antimicrobials is established, there is a need to develop pharmaceutically acceptable formulations that may enhance the antibacterial effectiveness. In fact, the pressing need to find antimicrobials with new modes of action that obviate microbial resistance is widely recognized [42]. In the present work, we set out to explore the antibacterial action of compositions prepared by solvent-free co-grinding of βCD (a widely used excipient in pharmaceutical formulations) with ALF062.

2. Experimental

2.1. Starting materials and chemicals

$Mo(CO)_6$ (Sigma-Aldrich), tetraethylammonium bromide (Sigma-Aldrich, 98%), diethylene glycol dimethyl ether (Fluka, 99%), β-cyclodextrin (kindly donated by Laboratories La Rouquette, France, water content 10 mol/mol), myoglobin from equine skeletal muscle (Sigma-Aldrich, 95–100%, lyophilized powder), sodium dithionite (Sigma-Aldrich, ≥82%), and phosphate buffered saline tablets (Sigma-Aldrich), were purchased from commercial sources and used as received.

2.2. Instrumentation

Microanalyses (CHN) were obtained using a Leco TruSpec CHNS 630–200–200 analyzer (Leco, Saint Joseph, MI, USA). FT-IR spectra (KBr disks) were collected using a Unican Mattson 7000 spectrometer (Mattson Instruments Inc., Madison, WI, USA) equipped with a DTGS CsI detector (resolution 4 cm^{-1}, 128 scans). Attenuated total reflectance (ATR) FT-IR spectra were measured on a Bruker Tensor 27 spectrometer (Bruker, Billerica, MA, USA) equipped with a Specac Golden Gate Mk II ATR accessory (Specac, Orpington, UK) having a diamond top plate and KRS-5 focusing lenses (resolution 4 cm^{-1}, 256 scans). FT-Raman spectra were recorded on a Bruker RFS-100 FT-spectrometer equipped with a Ni:YAG laser with an excitation wavelength of 1064 nm (resolution 4 cm^{-1}, 1000 scans). UV–Vis spectra for the Mb assays were collected using a GBC UV/Vis 918 Cintral spectrophotometer with a scan speed of 200 nm min^{-1} and a slit width of 2 nm. Powder X-ray diffraction (PXRD) data were collected at room temperature on a Malvern Panalytical Empyrean diffractometer (Malvern Panalytical, Malvern, UK) equipped with a spinning flat plate sample holder and a PIXcel 1D detector set at 240 nm from the sample, in a Bragg-Brentano para-focusing optics configuration. Cu-K$\alpha_{1,2}$ X-radiation (λ_1 = 1.540598 Å, λ_2 = 1.544426 Å) filtered with nickel foil was used, with the X-ray tube operated at the voltage of 45 kV and the current of 40 mA. Samples were step-scanned from 3 to 70° (2θ) with step sizes of 0.02° and a counting time of 50 s per step. Thermogravimetric analysis (TGA) was performed using a Shimadzu TGA-50 system at a heating rate of 5 °C min^{-1} under a nitrogen atmosphere. Ball milling (BM) was carried out in a TMAXCN Vertical Planetary Ball Mill machine (XQM Series), working at a velocity of 600 rpm.

2.3. Synthesis

2.3.1. $[NEt_4][Mo(CO)_5Br]$ (1)

Following the method reported for the synthesis of $[NEt_4][Mo(CO)_5Cl]$ [43], tetraethylammonium bromide (1.01 g, 4.80 mmol) was heated with an excess of $Mo(CO)_6$ (2.02 g, 7.65 mmol) in diethylene glycol dimethyl ether (30 mL) at 120 °C until the steady evolution of carbon monoxide stopped. The mixture was filtered hot under an atmosphere of nitrogen. Adding hexane to the cooled filtrate gave yellow crystals of **1**. After removal of the excess solvent by decantation, the crystals were washed with hexane, and finally dried under reduced pressure. Anal. Calcd. for $C_{13}H_{20}BrMoNO_5$: C, 35.00; H, 4.52; N, 3.14. Found: C, 34.68; H, 4.39; N, 3.08%. FT-IR (KBr, cm^{-1}): ν_{CO} = 2069 (w), 1908 (s), 1870 (s). These carbonyl stretching frequencies agree with those reported previously [44]. Raman (cm^{-1}): 2989 (w), 2951 (w), 2069 (m), 1971 (s), 1848 (m), 490 (w), 402 (w), 116 (s), 69 (s).

2.3.2. 1-βCD

A mixture of **1** (0.18 g, 0.40 mmol) and βCD (0.53 g, 0.40 mmol) was transferred to a 7 mL Teflon grinding jar containing three yttrium-doped zirconia milling balls with a diameter of 3 mm. As a matter of precaution, this procedure was performed in a glove box under an atmosphere of argon. The mixture was milled for 24 h at room temperature, giving a pale-yellow powder designated as **1**-βCD. Selected FT-IR (KBr, cm^{-1}): 3010 (w), 2989 (w), 2928 (m), 2069 (w, ν_{CO}), 1911 (s, ν_{CO}), 1871 (s, ν_{CO}), 1462 (w), 1408 (w), 1369 (w), 1335 (w), 1156 (m), 1080 (m), 1030 (s), 946 (m), 858 (w), 799 (w), 756 (w), 707 (w), 614 (m), 599 (s), 543 (m), 360 (s). Raman (cm^{-1}): 2992 (m), 2955 (m), 2906 (m), 2068 (m), 1971 (s), 1848 (s), 1462 (w), 946 (w), 489 (w), 402 (w), 115 (s), 69 (s). The PXRD pattern and TGA curve of **1**-βCD are provided in Figs. S5 and S6, respectively, in the Supplementary Information.

2.4. Myoglobin assay

CO release from **1** and **1**-βCD was studied spectrophotometrically and quantified by the standard myoglobin (Mb) assay which uses absorption spectroscopy to measure the conversion of deoxy-Mb to carbonmonoxy-myoglobin (COMb) [45]. The amount of COMb formed was determined at different times by recording absorption spectra in the Q-band region and monitoring the attenuation of the corresponding deoxy-Mb band ($\lambda_{max} = 557$ nm) and the growth of the two characteristic COMb bands ($\lambda_{max} = 540$ and 577 nm; Fig. S1 in the Supplementary Information). These spectral changes result from the decarbonylation of the CORM and the immediate binding of the released CO to the iron center of deoxy-Mb (rate constant, $k = 0.38$ μM s^{-1} [45]).

Stock solutions of Mb (~100 μM) and sodium dithionite (40 mg/mL) were freshly prepared in N_2-degassed 10 mM phosphate-buffered saline (PBS, pH 7.4). Under an atmosphere of nitrogen, these two stock solutions and 10 mM PBS were added to a sealed quartz cuvette (3500 μL) in the following order: 10 mM PBS (1185 μL), 100 μM Mb (1500 μL), 40 mg/mL sodium dithionite (300 μL). An absorption spectrum in the visible range (450–650 nm) was recorded for the resultant deoxy-Mb solution. Subsequently, 2 mM stock solutions of **1** in DMSO or **1**-βCD in PBS (15 μL) were added immediately to the solution of deoxy-Mb, giving a final concentration of **1** or **1**-βCD of 10 μM. The cell was kept at 37 °C in the dark, with constant magnetic stirring. All the assays were conducted over a period of 6 h. The incubation was interrupted in intervals of 30 min to measure visible absorption spectra. At the end of each assay, complete conversion of deoxy-Mb to COMb was ensured by bubbling CO gas through the liquid phase, and the spectrum of COMb was recorded. The actual concentration of Mb in the cell was then determined by using the known extinction coefficient of COMb at 540 nm (15.4 mM^{-1} cm^{-1}). The spectroscopic data were treated in the standard way by applying a correction at the 510 nm isosbestic point [45]. All the assays were carried out in triplicate.

2.5. Antibacterial studies

2.5.1. Bacterial strains and growth conditions

For the determination of minimum inhibitory concentrations (MICs) and minimum bactericidal concentrations (MBCs), *E. coli* ATCC 25922 was chosen. Stock bacterial cultures were maintained at 4 °C in Tryptic Soy Agar (TSA; Liofilchem, Roseto degli Abruzz, Italy). Before each assay, a bacterial colony was transferred to 30 mL of Tryptic Soy Broth (TSB; Liofilchem, Roseto degli Abruzz, Italy) and incubated overnight at 25 °C with stirring (120 rpm). Then, an aliquot of the formerly grown suspension was transferred to fresh medium and incubated under the previously described conditions until the stationary phase of approximately 10^9 colony forming units per mL (CFU mL^{-1}) was reached.

For the bacterial viability experiments, the genetically transformed *E. coli* Top10 [46] was selected as a rapid, sensitive, and cost-effective method to assess the bacterial viability. Light emission from bioluminescent bacteria is directly dependent on their metabolic activity and allows the bacterial inactivation to be monitored rapidly and in real-time, allowing the action of antimicrobial drugs that act quickly to be detected, which is not possible using the commonly used laborious plating techniques. Suspensions of the bioluminescent *E. coli* were stored in 10% glycerol at −80 °C. Before each assay, a stock solution of the bacteria was added to 30 mL of TSB with 100 mg mL^{-1} of ampicillin (Sigma Chemical, St. Louis, MO, USA) and 25 mg mL^{-1} of chloramphenicol (Sigma Chemical, St. Louis, MO, USA) and incubated overnight at 25 °C with stirring (120 rpm). Then, an aliquot of this culture (300 μL) was aseptically transferred to 30 mL of fresh TSB medium with antibiotics and grown overnight at 25 °C at 120 rpm.

The correlation between the bioluminescent signal (RLU) and the CFU mL^{-1} was evaluated. An overnight bacterial culture was serially diluted (10^{-1} to 10^{-7}) in PBS. Then, diluted and non-diluted solutions were simultaneously drop-plated (10 μL) in triplicate onto TSA medium and read in a luminometer (1.0 mL) (TD-20/20 Luminometer, Turner Designs, Inc., Madison, WI, United States) to access the bioluminescence signal between 350 and 650 nm. The correlation results are shown in Fig. S2 in the Supplementary Information.

2.5.2. Determination of MICs and MBCs

The determination of the MICs and MBCs was performed using the microdilution assay described by ISO 20776-1 (2019) [47]. Before each assay, the overnight bacterial culture was diluted in TSB adjusted to 0.5 McFarland Standard, which corresponds to ~10^8 CFU mL^{-1}.

Fresh solutions of **1** (6.4 mM, dissolved in DMSO) and **1**-βCD (1.6 mM, dissolved in PBS) were added to bacterial suspension obtaining the final concentrations of 25, 50, 100, 200, 400 and 800 μM. For each experiment, two controls were included in parallel with treated samples: the bacterial growth control made with bacterial culture and PBS, and a solvent control made with bacterial culture and 6.25% (*v/v*) DMSO, representing the highest concentration of DMSO used in treated samples. An additional control was performed using the native βCD with concentrations between 1.0 and 4.0 mM to assess whether the cyclodextrin alone presented any bacterial effect. Controls and treated samples were incubated at 37 °C for 24 h. After this period, the turbidity of the suspensions and the number of viable cells were determined to calculate MIC and MBC values. The MIC is the lowest concentration of the complex that did not show a visible bacterial growth (no visible turbidity). The MBC is defined as the lowest concentration of complex that did not show any bacterial growth (no viable cells observed). For the bacterial cell quantification, the content of all the wells was serially diluted in PBS and drop-plated in triplicate (10 μL each drop) onto TSA plates. After 18 h of incubation at 37 °C, the colonies were counted at the most appropriate dilution, and the viable bacterial density was determined as log CFU mL^{-1}. At least three independent assays were performed for each condition and the results were averaged.

2.5.3. Bacterial viability

To evaluate the effect of **1** and **1**-βCD on the inactivation kinetics of *E. coli* Top10 [46,48], both substances were tested at the MBC determined in this study (400 μM). The concentration of an overnight bacterial culture was adjusted in TSB to the same values of OD_{600} as described above, corresponding to 10^8 of RLU. The bacterial suspension (750 μL) was transferred to Eppendorf tubes and incubated with **1** and **1**-βCD solutions (750 μL) to a final concentration of 400 μM. Growth and solvent controls were also included in this experiment. To access the effect of **1** and **1**-βCD on *E. coli* Top10 over time, the bioluminescence signal was measured after 0, 5, 10, 15 and 30 min of incubation at 25 °C, with orbital stirring (120 rpm) and the results are expressed as log RLU. Simultaneously, aliquots of treated samples and controls (100 μL) were collected at time 0 and whenever the detection limit of the luminometer was reached (2.75 log of RLU), serially diluted and pour-plated in duplicate onto TSA. The plates were incubated as previously described and the bacterial concentration expressed as CFU mL^{-1}. Three independent assays were performed for each condition and the results were

averaged.

2.5.4. Statistical analysis

Statistical analysis was performed using GraphPad Prism 9 software (San Diego, CA, USA). Normal distributions were checked with the Kolmogorov–Smirnov test, and the homogeneity of variance was accessed with the Brown–Forsythe test. The antimicrobial activity of compounds was evaluated by comparing the differences in the bacterial concentration between each treatment and the corresponding controls. For MICs and MBCs, the significances of the differences among the tested conditions were assessed using one-way analysis of variance (ANOVA) and Dunnet's multiple comparison tests. In the bacterial viability experiments, two-way ANOVA followed by Tukey's multiple comparison tests were applied to analyze the data. A value of $p < 0.05$ was considered significant.

3. Results and discussion

3.1. Characterization of 1-βCD

The grinding of drug/cyclodextrin mixtures can lead to different outcomes depending on the duration and intensity of grinding and on the physicochemical properties of the drug and CD. With weakly interacting components, physical mixtures or homogeneous solid dispersions may be formed, or the CD may promote a reduction in drug aggregation/agglomeration and/or particle size. Decreases in the degree of crystallinity of the drug (and/or CD) may range from minor to major, with the latter comprising partial or complete amorphization, which may be accompanied by inclusion complex formation in the case of more strongly interacting components. Ball-milling of a mixture of **1** and βCD in a 1:1 molar ratio for 24 h at room temperature produced an intimate physical mixture on the evidence of FT-IR spectroscopy, Raman spectroscopy, PXRD and TGA. Thus, the vibrational spectra (Figs. S3 and S4 in the Supplementary Information) and PXRD pattern (Fig. S5) of **1**-βCD can essentially be interpreted as a superposition of the spectra and patterns for each component. No significant shifts of the main vibrational bands or XRD Bragg reflections of **1** were observed in the co-ground product. A slight broadening of the XRD reflections of **1** was observed, indicating a small reduction in the degree of crystallinity. In accordance with the vibrational spectra and PXRD data, the TGA curve of **1**-βCD displays weight loss steps that can be attributed to the separate components (Fig. S6). Complex **1**, in its bulk crystalline state, exhibits a weight loss step of 17.5% between 100 and 150 °C, corresponding to partial decarbonylation (Step 1). Complete decarbonylation and decomposition of the tetraethylammonium ions then takes place between about 200 and 275 °C (Step 2). For **1**-βCD, individual steps are observed for the loss of water from the CD phase (from ambient temperature to 100 °C) and CO from the pentacarbonyl complex (from 100 to 150 °C, corresponding to Step 1). The next event, i.e., further decarbonylation coupled with decomposition of the $[NEt_4]^+$ ions (Step 2), triggers decomposition of the βCD component at a lower temperature (ca. 45 °C lower) than that observed for pure βCD.

ATR FT-IR spectra obtained for **1**-βCD at different times over a period of 90 d after its preparation showed that the incorporated pentacarbonyl complex is stable when the solid is stored under an inert atmosphere (Fig. S7 in the Supplementary Information). Similar tests with pure **1** under air over a period of 1 week showed that the complex is stable, with no difference between solids kept in the dark or under ambient light (Fig. S8).

3.2. CO release kinetics

The CO release properties of pure **1** and **1**-βCD under simulated biological conditions (PBS, pH 7.4, 37 °C) were investigated by the Mb-based spectrophotometric assay, considered the gold standard to analyze CO release from CORMs in vitro. In this assay, a degassed PBS solution of Mb (final concentration ca. 50 μM) from equine skeletal muscle was freshly reduced with an excess of sodium dithionite under an atmosphere of nitrogen. Solutions of **1** in DMSO or **1**-βCD in PBS were prepared and immediately added to the solution of deoxy-Mb to give a final CORM concentration of 10 μM. As expected, decarbonylation of **1** (free form) was spontaneous, being triggered by the interaction of the complex with water and the resultant hydrolysis of the Mo−Br bond [49]. Under our conditions, the decarbonylation reached a maximum of 3.23 mmol CO per mmol of complex after 300 min of incubation, corresponding to a CO releasing efficiency of 65% (Fig. 1). The half-life ($t_{1/2}$) of CO release, defined as the time taken to produce a COMb concentration of 5.0 μM, was ca. 6 min, while the time taken to release one equivalent of CO (based on Mo; t_1) was ca. 17 min. These values are somewhat shorter than those determined by Lynam and co-workers under slightly different Mb assay conditions ([Mb] ca. 60 μM, [1]= 40 μM, PBS, pH = 7.4, 37.8 °C; $t_{1/2}$ = 15 min; t_1 ca. 54 min) [49]. CO release data reported for **1** are compared in Table 1 and emphasize that the complex releases CO at different rates and in different amounts depending on a series of experimental variables such as the CORM concentration, solvent, medium, and presence of O_2 or other oxidant (i.e., peroxides).

In the mechanism proposed by Lynam and co-workers for water-triggered CO release from the complexes $[M(CO)_5X]^-$ (M = Cr, Mo, W; X = Cl, Br, I) (based on experimental studies with the complexes with M = Cr and X = Cl, Br), the initial hydrolysis step gives the coordinatively unsaturated fragment $\{M(CO)_5\}$, which may react reversibly with $[M(CO)_5X]^-$ to give $[\{M(CO)_5\}_2(\mu\text{-}X)]^-$ [49]. CO release could then take place through dissociation of CO from the dinuclear complex and/or the pentacarbonyl fragment. The liberated CO could be captured by $[M(CO)_5X]^-$ or $[\{M(CO)_5\}_2(\mu\text{-}X)]^-$ to give $M(CO)_6$ (and $[M(CO)_5X]^-$ in the case of the dinuclear complex), or by the protein in the Mb assay to give COMb. Accordingly, we confirmed that the treatment of **1** with N_2-degassed water (under an atmosphere of nitrogen) led within 5–6 h to the precipitation of $Mo(CO)_6$ (Fig. S8 in the Supplementary Information). The precipitation of the hexacarbonyl occurred more rapidly (within ca. 1 h) when the reaction was performed in non-degassed water under air. EPR studies showed that hydroxyl radicals are generated when **1** is immersed in an aqueous aerobic medium [50]. In the proposed mechanism [50], the initial step is the dissociation of Br^- to give a solvent stabilized $\{M(CO)_5\}$ fragment. This is followed by coordination of O_2 in the vacant position, protonation of the resultant superoxo

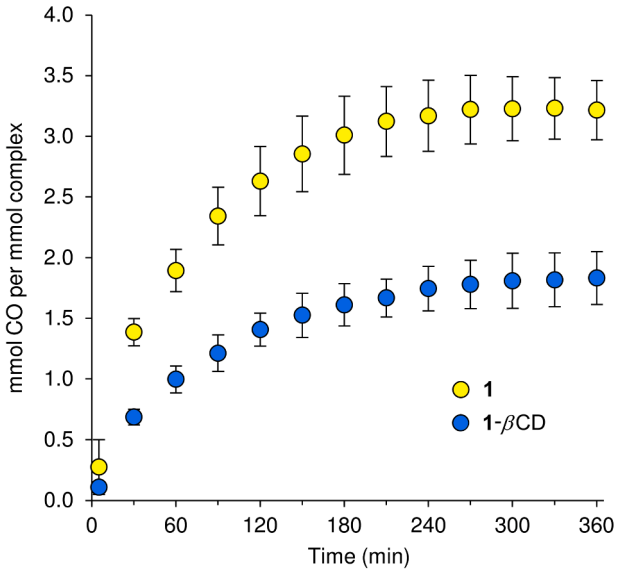

Fig. 1. CO-release profiles for **1** and **1**-βCD (10 μM) determined by the Mb assay.

Table 1
Comparison of CO release data for $[NEt_4][Mo(CO)_5Br]$ (**1**) and **1**-βCD.

CO quantification	Medium	Air/N_2	T/ °C	Solubility[a]	[1](μM)	t (min)	Equiv. CO/CO_2[b]	$t_{1/2}$ (min)[c]	Ref.
Mb assay	50 μM Mb, 0.4% $Na_2S_2O_4$, 0.5% DMSO, PBS7.4	N_2	37	soluble	10	300	3.23CO	6	This work
Mb assay	50 μM Mb, 0.4% $Na_2S_2O_4$, PBS7.4	N_2	37	soluble	10[d]	360	1.83CO	19	This work
Mb assay	60 μM Mb, 0.1% $Na_2S_2O_4$, 0.5% DMSO, PBS7.4	ns[e]	37.8	soluble	20	92	0.42CO[f]	41[g]	[49]
Mb assay	60 μM Mb, 0.1% $Na_2S_2O_4$, 0.5% DMSO, PBS7.4	ns[e]	37.8	soluble	40	60	1.0CO[f]	15	[49]
Mb assay	55 μM Mb, 0.1% $Na_2S_2O_4$, 1.7% DMSO, PBS7.4	air	rt	soluble	51	120	0.73CO	14	[50]
Mb assay	57 μM Mb, 0.1% $Na_2S_2O_4$, PBS7.4	air	rt	soluble	50	120	0.25CO	27,939	[50]
GC-headspace	RPMI[h]	air	37	sp. soluble	ca. 10^3	360	2.4CO	–	[50]
GC-headspace	Minimal salts medium	air	rt	ns	ns	240	3.8CO	–	[39]
GC-headspace	TBHP[i] (100:1[j]), H_2O	N_2	rt	ns	10^3–10^4	300	3.9CO+1.1(CO_2)	–	[50]
GC-headspace	TBHP (10:1[j]), decane, CH_2Cl_2	N_2	rt	soluble	10^3–10^4	180	4.9CO+0.2(CO_2)	–	[50]
GC-headspace	H_2O_2 (100:1[j]), H_2O	N_2	rt	ns	10^3–10^4	300	1.5CO+0.9(CO_2)	–	[50]
oximetry - COHb	Sheep blood, 4.8% MeOH	air	37	soluble	700–1400	75	5CO	–	[50]

[a] sp. = sparingly.
[b] Equivalents of CO and CO_2 released to the gas phase (GC-headspace) or transferred to protein (oximetry-COHb and Mb assay).
[c] Half-life of CO-release, unless otherwise indicated.
[d] **1**-βCD.
[e] ns = not specified. Solutions were overlaid with mineral oil to prevent the myoglobin being oxygenated.
[f] Plateau not reached.
[g] Time required to form 5 μM COMb (i.e., $t_{1/4}$).
[h] RPMI = tissue culture medium (RPMI-1630) supplemented with 10% fetal bovine serum.
[i] TBHP = *tert*-butylhydroperoxide.
[j] Initial oxidant:**1** molar ratio.

complex, and breaking of the O−O bond in the Mo−O−OH species to form a hydroxyl radical and an oxomolybdenum (Mo=O) species. Hence, the final stages in the decomposition of **1** under aerobic conditions are presumed to involve oxidation by O_2 with CO release from Mo species in higher oxidation states, leading eventually to total liberation of CO and formation of molybdates and/or polyoxomolybdates [50]. This is what happens when **1** is incubated in sheep blood under air, with oximetry showing that all 5 equivalents of CO are delivered to blood Hb within 75 min at 37 °C (Table 1) [50].

CO release from **1**-βCD reached a maximum of 1.83 mmol CO per mmol of Mo ($t_{1/2}$ ca. 19 min) after 360 min of incubation, corresponding to a CO-releasing efficiency of 37%. Native βCD, which has no carbonyl groups, was selected as a negative control. It did not cause any change in the spectrum of Mb, showing that the concentration of deoxy-Mb was maintained constant. The results show that under the conditions of the Mb assay the cyclodextrin has a braking effect on the kinetics of CO release from the complex $[Mo(CO)_5Br]^-$, as well as reducing the CO release efficiency. The different behaviors are reflected in the initial CO release rates: 3.6 ± 0.8 $mol_{CO}\ mol_{Mo}^{-1}\ h^{-1}$ for **1** *vs*. 1.6 ± 0.3 $mol_{CO}\ mol_{Mo}^{-1}\ h^{-1}$ for **1**-βCD. Since **1** is only sparingly soluble in water, DMSO is used as a cosolvent in the Mb assay to dissolve the complex. In contrast, **1**-βCD is soluble in water, and hence both components dissolve in PBS solution, eliminating the need to use an organic cosolvent. The apparent solubilizing effect of βCD on **1** may be due to an interaction or even complex formation in solution [35], which could make the pentacarbonyl complex less susceptible to hydrolysis of the Mo−Br bond, thereby leading to lower CO release rate and efficiency.

3.3. Antibacterial activity

The antibacterial activity of complex **1** and **1**-βCD was first evaluated by determining the MICs and MBCs. This assay involved the use of the compounds in a range of concentrations between 25 and 800 μM in an aerobic culture of *E. coli* ATCC 25922 growing in TSB. The results showed that both complexes exhibit an MBC value of 400 μM and an MIC value of 200 μM (ANOVA, $p < 0.05$) (Fig. 2). A compound is generally considered to be bactericidal if the MBC/MIC ratio is less than 4 [51], so the ratio of 2 for these compounds against *E. coli* cells indicates bactericidal rather than bacteriostatic activity. When the native βCD was tested alone at concentrations between 1.0 and 4.0 mM, after 24 h of incubation the suspension turbidity was similar to the bacteria growth control (ANOVA, $p > 0.05$), indicating that βCD does not have any antibacterial effect against *E. coli* per se.

For comparison, Saraiva and co-workers found that **1** presented an MBC value of 600 μM and an MIC value of 450 μM (MBC/MIC = 1.3) against *E. coli* K12 MG1655 grown in minimal salts medium (OD_{600} = 0.01) [40].

The *E. coli* viability incubated in the presence of **1** and **1**-βCD was also evaluated over time using the genetically modified bioluminescent *E. coli* Top10. As both **1** and **1**-βCD act quickly, the bioluminescence method, rather than the conventional laborious plating method, was used to evaluate their action against *E. coli*. As shown in Fig. 3, after treatment with **1** and **1**-βCD, both substances rapidly decreased the viability of *E. coli*. At time of 0 min, the compounds decreased already the *E. coli* viability 1.15 log RLU for **1** and 1.55 log RLU for **1**-βCD (ANOVA, $p < 0.05$). These results may be explained by the fact that both compounds release CO quickly in solution, so when bacteria came into contact with the solutions of the compounds, there were already active bactericide species (coordinatively unsaturated molybdenum carbonyl fragments [40]: see below) in solution. After an exposure of 15 min of the bacterium to the complexes, a viability decrease of 3 logs (99.9% of RLU reduction) was observed (ANOVA, $p < 0.05$), and after a further 15 min, the detection limit of the method was reached, which means that complex **1** and **1**-βCD exhibit fast and potent bactericidal activity. The bioluminescence in the bacterial growth control (BG) remained constant during all the period of treatment, indicating that the conditions of the experiment did not affect the viability of *E. coli* cells (ANOVA, $p > 0.05$), and the decrease of the viability in the samples is only due to the bactericidal properties of the compounds (ANOVA, $p > 0.05$).

There is no significant difference in the bactericidal properties between **1** and **1**-βCD (ANOVA, $p > 0.05$). This was somewhat unexpected, as the bactericidal activity of **1** has been shown to be dependent on CO release [39–41], and the Mb assays revealed different CO release kinetics for the two compounds. An important difference between the Mb and antimicrobial assays is that the former is performed under anaerobic conditions, while the latter are performed under aerobic conditions. Secondly, the Mb assay measures the release of free CO gas into the medium, while bactericidal activity may be dependent on the release of CO into the intracellular space, which may take place via the anchoring of coordinatively unsaturated fragments, $\{Mo(CO)_x\}$, to the cell walls [41]. Evidence for the accumulation of Mo from **1** in *E. coli* cells was obtained by inductively coupled plasma mass spectrometry analysis of

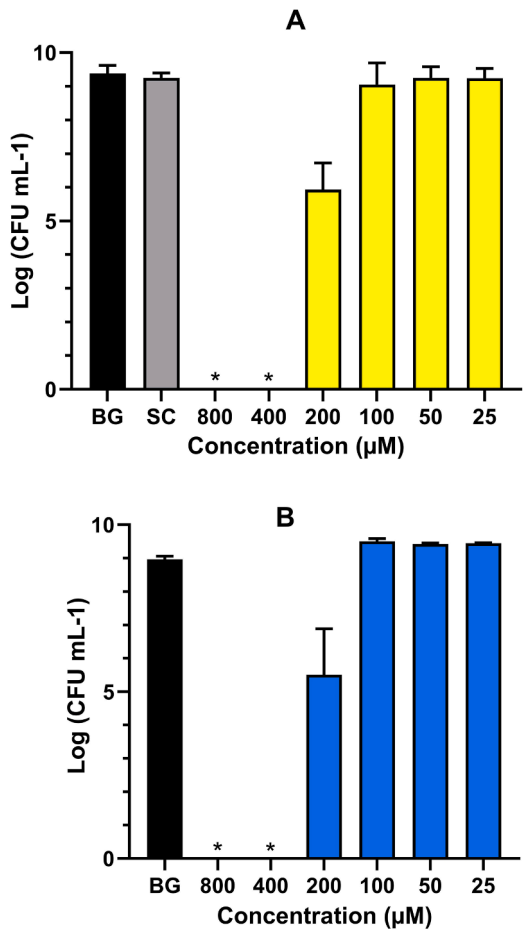

Fig. 2. Bactericidal effect of complex **1** (A) and **1**-βCD (B) against the growth of *E. coli* ATCC 25922. The solvent control (SC) was performed using the maximum amount of DMSO used in the bacterial viability experiments (BG). The data are representative of the mean and standard deviation of the values of at least three independent assays. Samples which reached the inactivation till the limit of the method are represented by (*). Concentration columns between 200 and 800 μM are statistically different from the BG and SC (ANOVA, $p < 0.05$).

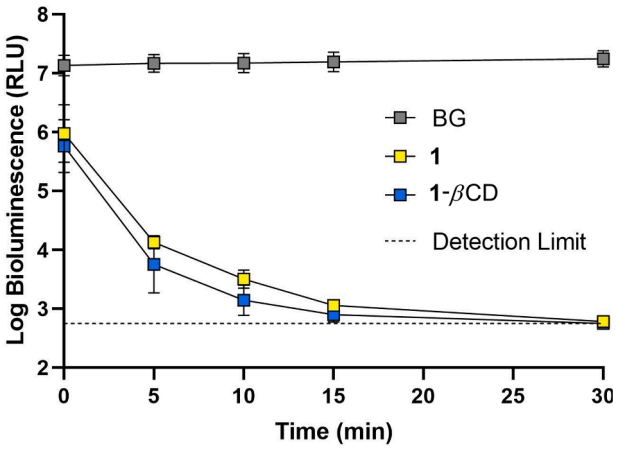

Fig. 3. Bioluminescence monitoring of bioluminescent *E. coli* Top10 treated with complexes **1** and **1**-βCD over time. The values are representative of the mean and standard deviation of at least three independent assays. Data from **1** and **1**-βCD are significantly different from BG (ANOVA, $p < 0.05$). The solid connecting lines are visual guides.

cells that had been incubated with the pentacarbonyl complex [40]. As mentioned in the introduction, the bactericidal activity of **1** and related CORMs has been linked with CO-dependent intracellular ROS bursts, which may be mediated by $\{Mo(CO)_x\}^0$ species in the presence of O_2 [40,41]. Hence, under these conditions, the influence of βCD, beyond conferring water solubility, may subside or vanish altogether, resulting in similar bactericidal activities.

4. Conclusion

This work aimed to examine β-cyclodextrin as an additive for dry co-grinding of $[Et_4N][Mo(CO)_5Br]$ (**1**) with a view to overcoming bioavailability issues related with the poor solubility of the pure CORM in aqueous media. Our studies have shown that ball-milling of **1** and βCD does not result in CORM amorphization nor inclusion complex formation, with only a small loss of crystallinity being observed for **1**. Nevertheless, when compared with the pure CORM, the mere presence of the β-cyclodextrin is sufficient to improve the in vitro dissolution characteristics of **1**. The solubility enhancement may be due to increased wettability of **1** (due to the intimate contact with the hydrophilic excipient) and/or CORM-CD interactions in solution. The presence of such interactions may explain why the CORM-CD system displays different CO release kinetics with respect to pure **1**, namely a lengthening of the half-life of CO release and a decrease in the CO release efficiency. Despite these effects, the presence of the CD does not appear to affect the bactericidal activity of the CORM against *E. coli* cells. The results indicate that βCD could be suitable as an excipient for the development of immediate-release formulations of CORMs like the pentacarbonyl complex **1**.

Declaration of Competing Interest

The authors declare that they have no known competing financial interests or personal relationships that could have appeared to influence the work reported in this paper.

Data availability

Data will be made available on request.

Acknowledgments

This work was developed within the scope of the project CICECO-Aveiro Institute of Materials (UIDB/50011/2020, UIDP/50011/2020 and LA/P/0006/2020), LAQV-REQUIMTE (UIDB/50006/2020 and UIDP/50006/2020), and CESAM (UIDB/50017/202 and UIDP/50017/2020), financed by national funds through the FCT (Fundação para a Ciência e a Tecnologia) / MCTES (Ministério da Ciência, Tecnologia e Ensino Superior) (PIDDAC). I.B.C. (ref. 2021.05953.BD), R.P.M. (ref. 2020.04758.BD), and C.V. (ref. SFRH/BD/150358/2019) are grateful to the FCT and the European Social Fund (ESF) for PhD grants. A.C.G. (CEECIND/02128/2017) thanks the FCT/MCTES for funding through the Individual Call to Scientific Employment Stimulus.

Supplementary materials

Supplementary material associated with this article can be found, in the online version, at doi:10.1016/j.jorganchem.2023.122844.

References

[1] T. Sjöstrand, Endogenous Formation of Carbon Monoxide in Man, Nature 164 (1949) 580–581, https://doi.org/10.1038/164580a0.
[2] R. Tenhunen, H.S. Marver, R. Schmid, The enzymatic conversion of heme to bilirubin by microsomal heme oxygenase, Proc. Natl. Acad. Sci. U. S. A. 61 (1968) 748–755, https://doi.org/10.1073/pnas.61.2.748.

[3] G.S. Marks, J.F. Brien, K. Nakatsu, B.E. McLaughlin, Does carbon monoxide have a physiological function? Trend. Pharmacol. Sci. 12 (1991) 185–188, https://doi.org/10.1016/0165-6147(91)90544-3.

[4] A. Verma, D.J. Hirsch, C.E. Glatt, G.V. Ronnett, S.H. Snyder, Carbon monoxide: a putative neural messenger, Science 259 (1993) 381–384, https://doi.org/10.1126/science.7678352.

[5] S.W. Ryter, L.E. Otterbein, Carbon monoxide in biology and medicine, BioEssays 26 (2004) 270–280, https://doi.org/10.1002/bies.20005.

[6] C. Peers, D.S. Steele, Carbon monoxide: a vital signalling molecule and potent toxin in the myocardium, J. Mol. Cell. Cardiol. 52 (2012) 359–365, https://doi.org/10.1016/j.yjmcc.2011.05.013.

[7] K. Ling, F. Men, W.-C. Wang, Y.-Q. Zhou, H.-W. Zhang, D.-W. Ye, Carbon monoxide and its controlled release: therapeutic application, detection, and development of carbon monoxide releasing molecules (CORMs), J. Med. Chem. 61 (2018) 2611–2635, https://doi.org/10.1021/acs.jmedchem.6b01153.

[8] H.-I. Choi, A. Zeb, M.-S. Kim, I. Rana, N. Khan, O.S. Qureshi, C.-W. Lim, J.-S. Park, Z. Gao, H.-J. Maeng, J.-K. Kim, Controlled therapeutic delivery of CO from carbon monoxide-releasing molecules (CORMs), J. Control. Release 350 (2022) 652–667, https://doi.org/10.1016/j.jconrel.2022.08.055.

[9] X. Ji, K. Damera, Y. Zheng, B. Yu, L.E. Otterbein, B. Wang, Toward carbon monoxide-based therapeutics: critical drug delivery and developability issues, J. Pharm. Sci. 105 (2016) 406–416, https://doi.org/10.1016/j.xphs.2015.10.018.

[10] R. Siracusa, A. Schaufler, V. Calabrese, P.M. Fuller, L.E. Otterbein, Carbon monoxide: from poison to clinical trials, Trend. Pharmacol. Sci. 42 (2021) 329–339, https://doi.org/10.1016/j.tips.2021.02.003.

[11] U. Goebel, J. Wollborn, Carbon monoxide in intensive care medicine—Time to start the therapeutic application?!, ICMx 8 (2020), https://doi.org/10.1186/s40635-020-0292-8.

[12] T.R. Johnson, B.E. Mann, J.E. Clark, R. Foresti, C.J. Green, R. Motterlini, Metal carbonyls: a new class of pharmaceuticals? Angew. Chem. Int. Ed. 42 (2003) 3722–3729, https://doi.org/10.1002/anie.200301634.

[13] R. Motterlini, J.E. Clark, R. Foresti, P. Sarathchandra, B.E. Mann, C.J. Green, Carbon monoxide–releasing molecules. Characterization of biochemical and vascular activities, Circ. Res. 90 (2002) e17–e24, https://doi.org/10.1161/hh0202.104530.

[14] R. Foresti, J. Hammad, J.E. Clark, T.R. Johnson, B.E. Mann, A. Friebe, C.J. Green, R. Motterlini, Vasoactive properties of CORM-3, a novel water-soluble carbon monoxide-releasing molecule, British J. Pharmacol. 142 (2004) 453–460, https://doi.org/10.1038/sj.bjp.0705825.

[15] R. Motterlini, P. Sawle, J. Hammad, R. Alberto, R. Foresti, C.J. Green, CORM-A1: a new pharmacologically active carbon monoxide-releasing molecule, FASEB J. 19 (2005) 284–286, https://doi.org/10.1096/fj.04-2169fje.

[16] R. Alberto, R. Motterlini, Chemistry and biological activities of CO-releasing molecules (CORMs) and transition metal complexes, Dalton Trans. (2007) 1651–1660, https://doi.org/10.1039/B701992K.

[17] C.C. Romão, W.A. Blätter, J.D. Seixas, G.J.L. Bernardes, Developing drug molecules for therapy with carbon monoxide, Chem. Soc. Rev. 41 (2012) 3571–3583, https://doi.org/10.1039/C2CS15317C.

[18] S. García-Gallego, G.J.L. Bernardes, Carbon-monoxide-releasing molecules for the delivery of therapeutic CO in vivo, Angew. Chem. Int. Ed. 53 (2014) 9712–9721, https://doi.org/10.1002/anie.201311225.

[19] A. Ismailova, D. Kuter, D.S. Bohle, I.S. Butler, An overview of the potential therapeutic applications of CO-releasing molecules, Bioinorg. Chem. Appl. (2018), 8547364, https://doi.org/10.1155/2018/8547364.

[20] N. Abeyrathna, K. Washington, C. Bashur, Y. Liao, Nonmetallic carbon monoxide releasing molecules (CORMs), Org. Biomol. Chem. 15 (2017) 8692–8699, https://doi.org/10.1039/c7ob01674c.

[21] Q. Min, X. Ji, Strategies toward metal-free carbon monoxide prodrugs: an update, ChemMedChem 18 (2023), e202200500, https://doi.org/10.1002/cmdc.202200500.

[22] P.C. Ford, Metal complex strategies for photo-uncaging the small molecule bioregulators nitric oxide and carbon monoxide, Coord. Chem. Rev. 376 (2018) 548–564, https://doi.org/10.1016/j.ccr.2018.07.018.

[23] T. Slanina, P. Šebej, Visible-light-activated photoCORMs: rational design of CO-releasing organic molecules absorbing in the tissue-transparent window, Photochem. Photobiol. Sci. 17 (2018) 692–710, https://doi.org/10.1039/c8pp00096d.

[24] A. Carné-Sánchez, F.J. Carmona, C. Kim, S. Furukawa, Porous materials as carriers of gasotransmitters towards gas biology and therapeutic applications, Chem. Commun. 56 (2020) 9750–9766, https://doi.org/10.1039/D0CC03740K.

[25] H. Yan, J. Du, S. Zhu, G. Nie, H. Zhang, Z. Gu, Y. Zhao, Emerging delivery strategies of carbon monoxide for therapeutic applications: from CO gas to CO releasing nanomaterials, Small 15 (2019), 1904382, https://doi.org/10.1002/smll.201904382.

[26] J. Hamman, J. Steenekamp, Excipients with specialized functions for effective drug delivery, Exp. Opin. Drug Deliv. 9 (2012) 219–230, https://doi.org/10.1517/17425247.2012.647907.

[27] J. van der Merwe, J. Steenekamp, D. Steyn, J. Hamman, The role of functional excipients in solid oral dosage forms to overcome poor drug dissolution and bioavailability, Pharmaceutics 12 (2020) 393, https://doi.org/10.3390/pharmaceutics12050393.

[28] T. Loftsson, M.E. Brewster, Cyclodextrins as functional excipients: methods to enhance complexation efficiency, J. Pharm. Sci. 101 (2012) 3019–3032, https://doi.org/10.1002/jps.23077.

[29] C. Muankaew, T. Loftsson, Cyclodextrin-based formulations: a non-invasive platform for targeted drug delivery, Basic Clin. Pharmacol. Toxicol. 122 (2018) 46–55, https://doi.org/10.1111/bcpt.12917.

[30] L. Ferreira, J. Campos, F. Veiga, C. Cardoso, A.C. Paiva-Santos, Cyclodextrin-based delivery systems in parenteral formulations: a critical update review, Eur. J. Pharm. Biopharm. 178 (2022) 35–52, https://doi.org/10.1016/j.ejpb.2022.07.007.

[31] M. Jug, P.A. Mura, Grinding as solvent-free green chemistry approach for cyclodextrin inclusion complex preparation in the solid state, Pharmaceutics 10 (2018) 189, https://doi.org/10.3390/pharmaceutics10040189.

[32] S.B. Carneiro, F.Í.C. Duarte, L. Heimfarth, J.S.S. Quintans, L.J. Quintans-Júnior, V. F.V. Júnior, Á.A.N. Lima, Cyclodextrin–drug inclusion complexes: in vivo and in vitro approaches, Int. J. Mol. Sci. 20 (2019) 642, https://doi.org/10.3390/ijms20030642.

[33] M. Messner, S.V. Kurkov, P. Jansook, T. Loftsson, Self-assembled cyclodextrin aggregates and nanoparticles, Int. J. Pharm. 387 (2010) 199–208, https://doi.org/10.1016/j.ijpharm.2009.11.035.

[34] M.B. Jesus, L.F. Fraceto, M.F. Martini, M. Pickholz, C.V. Ferreira, E. Paula, Non-inclusion complexes between riboflavin and cyclodextrins, J. Pharm. Pharmacol. 64 (2012) 832–842, https://doi.org/10.1111/j.2042-7158.2012.01492.x.

[35] M.J. Arias, J.R. Moyano, J.M. Ginés, Investigation of the triamterene–β-cyclodextrin system prepared by co-grinding, Int. J. Pharm. 153 (1997) 181–189, https://doi.org/10.1016/S0378-5173(97)00101-4.

[36] C.C. Romão, S.S. Rodrigues, J.D. Seixas, A.R.M. Pina, B. Royo, A.C. Fernandes, I. Gonçalves, W. Haas, Method for Treating a Mammal by Administration of a Compound Having the Ability to Release CO, WIPO (PCT) Patent WO 2007/073226 A1, 2007.

[37] L.K. Wareham, R.K. Poole, M. Tinajero-Trejo, CO-releasing metal carbonyl compounds as antimicrobial agents in the post-antibiotic era, J. Biol. Chem. 290 (2015) 18999–19007, https://doi.org/10.1074/jbc.R115.642926.

[38] J. Cheng, J. Hu, Recent advances on carbon monoxide releasing molecules for antibacterial applications, ChemMedChem 16 (2021) 3628–3634, https://doi.org/10.1002/cmdc.202100555.

[39] L.S. Nobre, J.D. Seixas, C.C. Romão, L.M. Saraiva, Antimicrobial action of carbon monoxide-releasing compounds, Antimicrob. Agents Chemother. 51 (2007) 4303–4307, https://doi.org/10.1128/AAC.00802-07.

[40] A.F.N. Tavares, M. Teixeira, C.C. Romão, J.D. Seixas, L.S. Nobre, L.M. Saraiva, Reactive oxygen species mediate bactericidal killing elicited by carbon monoxide-releasing molecules, J. Biol. Chem. 286 (2011) 26708–26717, https://doi.org/10.1074/jbc.M111.255752.

[41] L.S. Nobre, H. Jeremias, C.C. Romão, L.M. Saraiva, Examining the antimicrobial activity and toxicity to animal cells of different types of CO-releasing molecules, Dalton Trans. 45 (2016) 1455–1466, https://doi.org/10.1039/c5dt02238j.

[42] J. O'Neill, Tackling drug-resistant infections globally: final report and recommendations. Review on antimicrobial resistance, Wellcome Trust and HM Government, 2016.

[43] H. Liu, P. Wang, Q. Zhao, Y. Chen, B. Liu, B. Zhang, Q. Zheng, Syntheses, toxicity and biodistribution of CO-releasing molecules containing $M(CO)_5$ (M = Mo, W and Cr), Appl. Organomet. Chem. 28 (2014) 169–179, https://doi.org/10.1002/aoc.3105.

[44] E.W. Abel, I.S. Butler, J.G. Reid, The anionic halogenopentacarbonyls of chromium, molybdenum, and tungsten, J. Chem. Soc. 382 (1963) 2068–2070, https://doi.org/10.1039/jr9630002068.

[45] A.J. Atkin, J.M. Lynam, B.E. Moulton, P. Sawle, R. Motterlini, N.M. Boyle, M. T. Pryce, I.J.S. Fairlamb, Modification of the deoxy-myoglobin/carbonmonoxy-myoglobin UV-vis assay for reliable determination of CO-release rates from organometallic carbonyl complexes, Dalton Trans. 40 (2011) 5755–5761, https://doi.org/10.1039/C0DT01809K.

[46] E. Alves, C.M.B. Carvalho, J.P.C. Tomé, M.A.F. Faustino, M.G.P.M.S. Neves, A. C. Tomé, J.A.S. Cavaleiro, Â. Cunha, S. Mendo, A. Almeida, Photodynamic inactivation of recombinant bioluminescent *Escherichia coli* by cationic porphyrins under artificial and solar irradiation, J. Ind. Microbiol. Biotechnol. 35 (2008) 1447–1454, https://doi.org/10.1007/s10295-008-0446-2.

[47] ISO 20776-1, Clinical Laboratory Testing and In Vitro Diagnostic Test Systems - Susceptibility Testing of Infectious Agents and Evaluation of Performance of Antimicrobial Susceptibility Test Devices — Part 1: Broth Micro-Dilution Reference Method for testing the In Vitro Activity of Antimicrobial Agents Against Rapidly Growing Aerobic Bacteria Involved in Infectious Diseases, International Organization for Standardization, Geneva, Switzerland, 2019, p. 2019.

[48] C. Vieira, A.T.P.C. Gomes, M.Q. Mesquita, N.M.M. Moura, M.G.P.M.S. Neves, M.A. F. Faustino, A. Almeida, An insight into the potentiation effect of potassium iodide on aPDT efficacy, Front. Microbiol. 9 (2018) 2665, https://doi.org/10.3389/fmicb.2018.02665.

[49] W.-Q. Zhang, A.J. Atkin, R.J. Thatcher, A.C. Whitwood, I.J.S. Fairlamb, J. M. Lynam, Diversity and design of metal-based carbon monoxide-releasing molecules (CO-RMs) in aqueous systems: revealing the essential trends, Dalton Trans. (2009) 4351–4358, https://doi.org/10.1039/b822157j.

[50] J.D. Seixas, Ph.D. Thesis, Instituto de Tecnología Química e Biológica da Universidade Nova de Lisboa, 2010.

[51] G.A. Pankey, L.D. Sabath, Clinical relevance of bacteriostatic versus bactericidal mechanisms of action in the treatment of gram-positive bacterial infections, Clin. Infect. Dis. 38 (2004) 864–870, https://doi.org/10.1086/381972.